

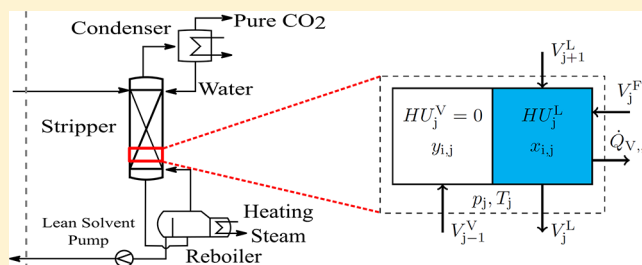
Dynamic Simulation and Investigation of the Startup Process of a Postcombustion-Capture Plant

Thomas Marx-Schubach* and Gerhard Schmitz

Institute of Engineering Thermodynamics, Hamburg University of Technology, Denickestrasse 17, 21073 Hamburg, Germany

Supporting Information

ABSTRACT: Carbon capture is an important possibility to reduce carbon dioxide emissions. To be able to study the startup process of such an amine-scrubbing process, a startup model of a postcombustion-capture plant (pcc-plant) was developed in the Modelica language and validated with measured data from a pilot plant in Heilbronn, Germany. Afterward, the process was scaled up in the model to handle the entire flue-gas flow of a 875 MW coal-fired power plant, resulting in three parallel capture plants. A case study was carried out to investigate the startup process of the pcc-plant in detail, indicating that the startup time increased drastically when the plant is operating at partial load. The startup time for a cold start from the beginning of steam flow to a 90% carbon-capture rate is $t = 1900$ s at full load and $t = 11\,075$ s at 15% load. The total heat demand in the reboiler of one pcc-plant is 326 GJ at full load and 370 GJ at 15% load. Other results show that the startup time increases linearly with increasing total amount of solvent and that the steam flow rate and solvent flow rate have a high impact on the startup time.



1. INTRODUCTION

Reduction of CO₂ emissions is essential in order to stop global warming and mitigate its effects. One important possibility to reduce CO₂ emissions besides the use of renewable energies is capturing CO₂ from flue gases of coal-fired power plants followed by compression and storage of the carbon dioxide in underground formations. Various carbon-capture technologies are available. The most mature technology is postcombustion capture.^{1,2}

Electricity generation from renewable energies leads to an increase in fluctuations in the power grid.³ Power plants have to be operated much more flexibly to compensate these fluctuations. Therefore, the amount of startup and shutdown sequences will also increase.⁴ To examine and optimize these dynamic periods and thus allow for efficient plant operation, the development of dynamic models is crucial. In this publication, a model of a postcombustion-capture plant (pcc-plant) is presented that can be used to simulate the startup process of a pcc-plant.

The postcombustion-capture process is expensive and energy intensive.⁵ In particular, the startup process requires a lot of energy. Hence, the development of startup models is important to gain a profound understanding of this complex process. The model can also be used to minimize the startup time or energy input in the future.

A large amount of publications on modeling of thermal-separation processes can be found in the literature. However, only a few deal with the simulation of thermal-separation startup processes in general or startup processes of pcc-plants in particular.

Ruiz et al.⁶ present a model for the simulation of startup processes of tray-distillation columns using an equilibrium model developed by Gani et al.⁷ The authors separate the startup process into different steps. This concept is often also used in the following publications. Kruse et al.⁸ developed an equilibrium model for the simulation of rectification-column startup processes. The model is validated in detail with their own experimental data.

Wang et al.⁹ simulated the startup process of a batch-distillation column. In contrast to the earlier publications, the model equations switch from a nonequilibrium state, where the equilibrium-condition and vapor-summation equations are not valid, to an equilibrium state. The switching occurs when the bubble pressure of the liquid mixture reaches the absolute pressure. Before the switching point, the vapor composition is equal to the bubble composition, and the pressure is fixed at the initial pressure.¹⁰ Reepmeyer et al.¹¹ used this equilibrium model of a rectification column to derive optimal startup strategies.

Forner^{12,13} chose a similar approach and extended the model to simulate the startup process of a reactive rectification column with different internals. He compared the startup processes of packed and tray columns and derived optimal startup strategies for both column types. The author concluded that for each column type, another optimal startup strategy has to be found.

Received: July 25, 2018

Revised: November 9, 2018

Accepted: November 12, 2018

Published: November 12, 2018

Elgue et al.¹⁴ developed a batch-distillation-column-startup model in two versions, a simplified one and a more complex one. The models were validated with experimental data. Niggemann et al.¹⁵ developed a startup model for a dividing-wall column using the Aspen Custom Modeler. Dietl¹⁰ presented an equilibrium model and a nonequilibrium model for the startup simulation of tray columns in Modelica.

Jayarathna et al.¹⁶ and Kvamsdahl et al.¹⁷ performed startup simulations of an absorption unit of a pcc-plant using a nonequilibrium-column model. Compared to those for normal plant operation, the equations of the model were not changed. This is only possible in the absorption unit, as the process is operated below the boiling point of the solution.¹⁸ Gaspar et al.¹⁹ also simulate the beginning of the startup process of a pcc-plant. The authors use a buffer tank to store part of the lean solvent to start up the absorption unit. They do not reveal whether they take into account the heatup process in the desorption unit.

Wellner¹⁸ closed this gap, developing an equilibrium model of a pcc-plant and simulating the startup process of the entire pcc-plant. Also, the startup of the stripper was simulated. The model was based on the model of Dietl,¹⁰ and it was validated with measured data from a pilot pcc-plant located in Heilbronn, Germany.

In this publication, the model from Wellner¹⁸ is used in an extended form. The same model was also used to find an optimal solvent-flow-rate trajectory during the startup process.²⁰

First, the process and startup procedure is described briefly. Afterward, the modeling development is described. The model is validated using measured data from a pilot pcc-plant in Heilbronn, Germany. As the startup process of the complete pcc-plant is not investigated in detail in the literature yet, the developed startup model is used to examine the influences of different parameters and input variables on the startup time. A scale-up process is performed using Aspen Plus, resulting in a pcc-plant at industrial scale used for this case study. The varied parameters and input variables are the steam flow rate into the reboiler, the solvent flow rate of the lean-solvent pump, the total amount of solvent, and the distribution of solvent in the pcc-plant.

2. PROCESS DESCRIPTION

For the capturing of carbon dioxide from flue gases of thermal power plants, different technologies can be used. The most important are precombustion, oxyfuel, and postcombustion technologies. In this publication, the postcombustion technology is used, as existing power plants can be retrofitted.¹ Furthermore, the postcombustion technique is the most mature, and the impact on the power plant is low compared with those from the others.¹ One drawback of the postcombustion technology is the typically low partial pressure of CO₂ in flue gases.

The postcombustion-capture technology can be realized using different processes, such as absorption, adsorption, or membrane processes. In this publication, a chemical absorption process using amines was chosen and investigated. The used solvent is an aqueous 30 wt % monoethanolamine (MEA) solution. In Figure 1, a simplified process-flow diagram of the process is illustrated.

The process can be described as follows. First, the flue gas is cooled to a temperature of approximately 35 °C in a flue-gas cooler. Additionally, sulfur dioxide is removed from the flue gas in the flue-gas cooler. The flue gas is compressed in a blower and

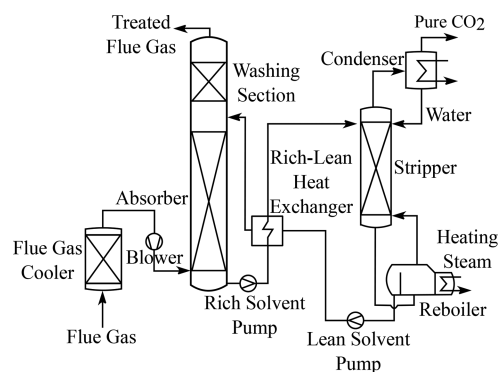


Figure 1. Process-flow diagram of a postcombustion-capture plant.²¹

flows upstream through the absorption unit, which is usually filled with random or structured packings. The solvent flows downstream in a counterflow through the absorption unit; the carbon dioxide is dissolved in the solvent and reacts mostly with the amine in the solution. Residue of the flue gas flows upstream through a washing section, where the amine residues are washed out of the flue gas. Afterward, it is discharged to the atmosphere. The rich solvent is collected in the absorption sump and pumped to the stripper through a heat exchanger, where it is preheated. In the reboiler of the stripper, the solvent is evaporated to achieve a regeneration of the solvent. Because of the increased temperature, the phase equilibrium between carbon dioxide in solution and gaseous carbon dioxide is shifted toward gaseous carbon dioxide. The gas flow upstream of the stripper is fed to the condenser, where most of the remaining steam is condensed. The CO₂ flow with a purity of over 99% can be compressed and stored in underground formations. The lean solution in the stripper sump is pumped back to the absorption unit.

Startup Procedure. The startup process of the pcc-plant is modeled in a simplified form. The model consists only of the components illustrated in Figure 2. All other components, such as additional solvent tanks or heat exchangers, pump for the solvent-makeup flow, and additional control structures are neglected for the sake of simplification. In contrast to Figure 1, the flue-gas cooler and the blower are also neglected in the model.

The startup process of the simplified plant runs as follows:

1. The solvent pumps are switched on to wet the columns and to get a homogeneous solvent mixture in the plant.
2. When the column packings are wetted, the flue gas is fed into the absorption unit.
3. As soon as the power plant is able to provide steam, the steam control valve to the reboiler is opened.
4. Once the desired reboiler temperature is reached, the reboiler temperature is controlled by the steam valve.
5. The startup process is finished when a carbon-capture rate of 90% is reached. In this publication, the carbon-capture rate is controlled using the lean-solvent pump.

3. MODEL DESCRIPTION

To examine and optimize the startup process and thus allow efficient capture-plant operation, the development of dynamic models is crucial.⁴

The model was developed using the acausal, equation-based, and object-oriented modeling language Modelica.²² The Modelica language is widely used in different fields of engineering, and the object-oriented approach gives the

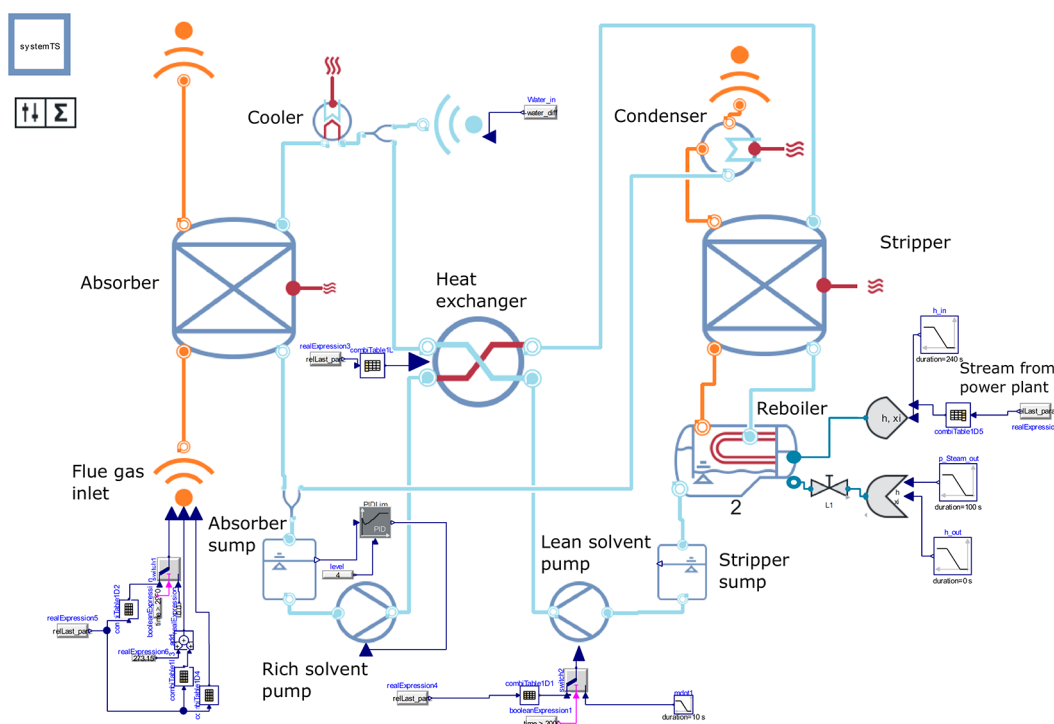


Figure 2. Modelica model of the pcc-plant in the Dymola simulation environment used for the case study.

opportunity to reuse and modify the developed models. Also, coupling to other models is possible, which is desirable in this case, especially coupling to power plants. In the Modelica language, several model libraries for conventional power plants have already been developed,^{23,24} and coupling to power-plant models has also already been performed.^{21,25} As a consequence, it is advantageous to use the Modelica language in this case. Simulations were carried out in the simulation environment Dymola developed from Dassault Systèmes.

The model of the pcc-plant was developed using the model library ThermalSeparation²⁶ and is based on the model developed by Wellner et al.^{18,21} The steam side of the reboiler was modeled using the ClaRa library.²³ During the modeling process the following assumptions were made:

- The vapor medium in the absorption unit consists of N_2 , O_2 , H_2O , and CO_2 . Other components, such as Ar, were neglected in the flue gas.
- The gas phase in the stripper and reboiler only consists of H_2O and CO_2 .
- The liquid medium consists of monoethanolamine (MEA), H_2O , and CO_2 in all components, and the substance MEA is considered to exist only in the liquid phase.
- All gas phases are assumed to behave like an ideal gas.
- The reactions and the phase equilibrium are calculated using the combined approach from Oexmann.²⁷
- The heat capacity and the liquid density of the solvent, as well as the heat of reaction of CO_2 in the solvent, are also calculated with correlations from Oexmann.²⁷
- Heat loss to ambience is neglected in all components.
- The pressure drop in the columns is calculated using a linear pressure approach with nominal values, and the liquid holdup in the columns is calculated using the correlation of Stichlmair.²⁸

- The calibration factor for the phase equilibrium in the absorption unit is the same as that in the model developed by Wellner.²¹ Reactions only take place in the stripper, absorber, and reboiler.

The basic equations used for the modeling of the columns are presented by Dietl^{10,29} and Wellner.¹⁸ The equations in the absorption unit were not changed, whereas the equations in the stripper model had to be adapted for startup operation. To model the startup process of the stripper, the process is divided into different steps. The resulting model is an advanced version of the startup model developed by Forner,^{12,13} which is only valid for reactive rectification columns, where all components in the feed are in a liquid state, and is not valid for gas-absorption processes, such as the carbon-capture process in this work. As a consequence, the model of Forner has to be extended. The steps are illustrated in Figure 3 for one column stage. The column is modeled using a 1D model and is discretized in the axial direction. Every column stage passes through all steps during the startup process, but not all column stages are necessarily in the same step at the same time.

At the beginning of the startup process, the column is in a cold and empty state (step A in every stage). The model is initialized at a constant pressure and temperature, normally at ambient pressure and temperature. The equilibrium condition is not valid. When the solvent pumps are switched on, liquid solvent enters the column stage at the top (step B). As soon as the maximum liquid hold up in the column stage is reached, the solvent begins to flow to the stage below (step C). Once the solvent evaporates in the reboiler or in the column stage below, the evaporated solvent begins to flow into the column stage (step D). The gas phase consists of water and carbon dioxide in the model. It is assumed that monoethanolamine only exists in the liquid phase. At this time, the temperature is still lower than the boiling temperature of the solvent. Therefore, it is assumed that the entering steam condenses immediately in the stage. It is

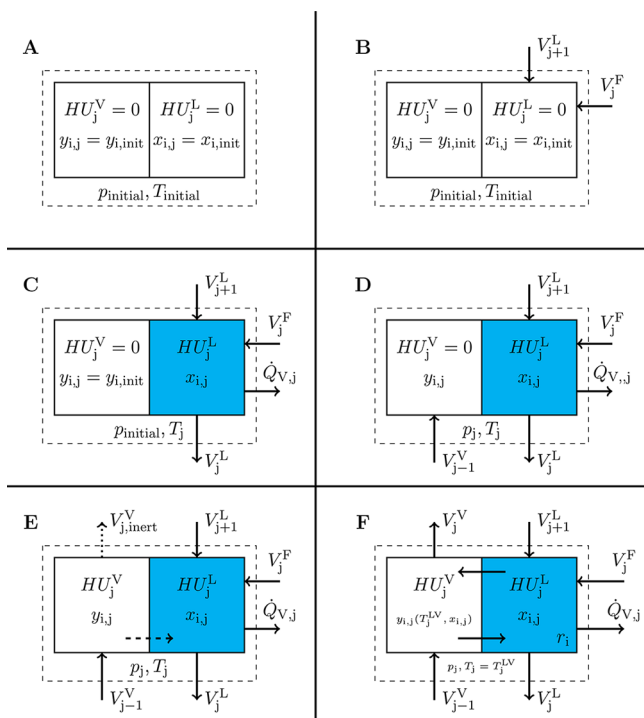


Figure 3. Schematic overview of different steps (A–F) in one column segment during the startup process (cf. Forner¹²).

also assumed that the carbon dioxide does not react with the solvent and flows upstream to the column head (step E). The stage is heated up by the condensing steam until the boiling temperature in the stage is reached. From that moment on, the equilibrium condition is valid for both vapor components (H_2O and CO_2), and the startup process is finished in this column stage (step F).

These steps are implemented in the model. For steps A–D, no switching of any equations is necessary. Between steps D and E as well as E and F, two equations are changed in the equation systems of every column stage.

The equilibrium condition is not valid at the beginning of the startup process. Therefore, the mass transfer over the phase boundary is prevented from setting the mole flow over the phase boundary to zero. Variable j indicates the column stage, and i indicates the component in the mixture.

$$\dot{N}_{j,i}^{\text{vap,trans}} = 0 \quad (1)$$

The pressure is fixed at ambient pressure during steps A–D.

$$p_j^{\text{sys}} = p_j^{\text{init}} \quad (2)$$

The switching condition between steps D and E is the beginning of vapor flow into the stage.

$$\dot{V}_{\text{in}}^{\text{vap}} > 0 \quad (3)$$

After switching, the pressure is not fixed at ambient pressure any longer. The system pressure corresponds to the vapor pressure, which is determined by the equation for the total amount of substance balance.

$$p_j^{\text{sys}} = p_j^{\text{init}} \rightarrow p_j^{\text{sys}} = p_j^{\text{v}} \quad (4)$$

The mole flow of CO_2 over the phase boundary is still set to zero. The steam entering the column condenses immediately in this stage.

$$\text{For } \text{CO}_2: \dot{N}_{j,i}^{\text{vap,trans}} = 0$$

$$\text{For } \text{H}_2\text{O}: \dot{N}_{j,i}^{\text{vap,trans}} = \dot{V}_{j-1,i}^{\text{vap,in}} \times c_{j-1,i}^{\text{vap,in}} \quad (5)$$

The switching condition between steps E and F is fulfilled when the bubble pressure of the solvent mixture reaches the absolute system pressure.

$$p^{\text{bub}} \geq p^{\text{sys}} \quad (6)$$

In step F, the equilibrium condition should be fulfilled. Therefore, it seems to be consistent to switch to the following equation, where y_{ji} is the mole fraction of component i in the vapor phase of stage j , and y_{ji}^* is the mole fraction at the phase boundary.

$$y_{j,i} = y_{j,i}^* \quad (7)$$

However, the resulting equation system cannot be solved.¹⁰ Hence, the equation is replaced by an approximate equilibrium condition.

$$\dot{N}_{j,i}^{\text{vap,trans}} = -K(y_{j,i} - y_{j,i}^*) \quad (8)$$

The parameter for K should be chosen as high as the solver allows, which minimizes the difference between y_{ji} and y_{ji}^* . The result is a good approximation of the equilibrium condition.

In Table S1 in the Supporting Information, an overview of the switching conditions and equations used in the different steps is given.

4. VALIDATION

Model validation is an important task to confirm the validity of the model. Therefore, the model was validated using data measured from a startup process of a pilot plant located in Heilbronn, Germany. The pilot plant can handle a flue-gas flow of $1500 \text{ N m}^3/\text{h}$. The height is 40 m for the absorber unit and 29 m for the stripper. The columns are filled with the packing material VSP-25.³⁰ Compared with the pcc-plant depicted in Figure 1, the absorption unit in the pilot plant is split up into two parts. Between both absorption units an intercooling of the solvent is performed. More information about the pilot plant can be found in Rieder et al.³¹ and Wellner et al.²¹

The following boundary conditions for the validation are set to match the pilot-plant data:

- the flue-gas flow rate, temperature, and composition at the absorber inlet and the solvent flow rate of the lean-solvent pump (a rich-solvent pump is used to control the absorption-sump level)
- the heat flow rate into the reboiler
- the initial total amount of solvent and also the distribution of the solvent
- the pressure at each column top

Pressure loss in the columns is adjusted using a linear-pressure-drop model with nominal values. The heat exchanger is modeled in a simplified way. The heat-transfer coefficient is set to match the temperature difference between the inlet temperature of the lean solvent and the outlet temperature of the rich solvent.

Only the initial solvent composition differs from the measurements of the pilot plant, which is the reason why the validation results differ from those of the previous publication.²⁰ The authors assume that the measurements of the solvent loadings are likely erroneous.

All depicted measured data, except the solvent loadings, were measured online during plant operation. The reliability of these results is high, as the most important values (e.g., temperatures and CO₂ concentrations in the gas phase) were measured using a redundant measurement system. The solvent loadings were determined differently. During pilot-plant tests, samples of the solvent were taken every 30 min out of the absorber (rich solvent) and stripper sump (lean solvent). Those samples were analyzed by titration afterward, which could explain the deviation. It is defined as the quotient of the amount of CO₂ and MEA in the solvent.

$$\alpha = \frac{n_{\text{CO}_2}}{n_{\text{MEA}}} \quad (9)$$

In Table 1, the measured solvent loadings at steady-state operation and full load are compared to the solvent loading in

Table 1. Comparison of Solvent Loadings of Two Different Models with Measurements during Regular Operation

| | measurement | Modelica model | Aspen model |
|------------------|-------------|----------------|-------------|
| rich loading | 0.456 | 0.511 | 0.504 |
| lean loading | 0.118 | 0.197 | 0.19 |
| working capacity | 0.338 | 0.314 | 0.314 |
| mean loading | 0.287 | 0.354 | 0.347 |

the Modelica model. The working capacity as shown in Table 1 is defined as the difference between rich and lean loadings.

$$\Delta\alpha = \alpha_{\text{rich}} - \alpha_{\text{lean}} \quad (10)$$

To confirm the results of the Modelica model, the results of an Aspen Plus model of the pilot plant are also presented. The difference between the models is low, whereas the measurements show a high deviation from the simulation results. Therefore, the initial solvent loading at the beginning of the startup process is set to the mean loading calculated by the Modelica model. It is assumed that the initial solvent loading is the same in every component as the solvent is mixed as a result of the circulation of the solvent pump at the beginning of the startup process.

The initial solvent composition is calculated using the mean loading and the molality of the solvent. The molality, b , is defined in the following way:

$$b = \frac{n_{\text{MEA}}}{m_{\text{H}_2\text{O}}} \quad (11)$$

The molality of the solvent in the pilot plant is 7. The absorption unit is modeled with 20 equilibrium stages (5 below the intercooling unit and 15 above). The stripper comprises 10 equilibrium stages.

In the following, some important results of the validation are shown. At time $t = 0$ s, the flue-gas flow into the absorption unit is started. Steam flow into the reboiler is started with a short delay at time $t = 240$ s, and the solvent flow is started approximately 1 h before the flue-gas flow. The pilot plant is started from cold state to full-load operation. The solvent flow rate, flue-gas flow rate, and steam flow rate are constantly set to their steady-state values at full load of the plant during startup. In

Figure 4, the simulation results of the carbon-capture rate and the CO₂ flow upstream of the stripper are compared with

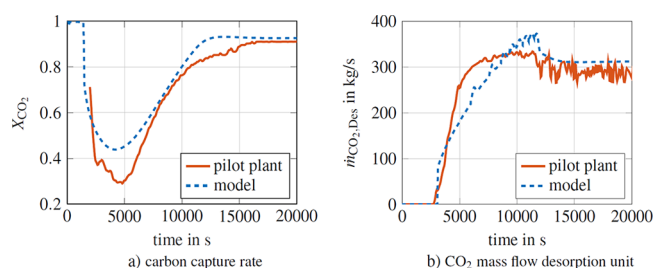


Figure 4. Validation results: (a) carbon-capture rate and (b) desorbed CO₂-mass flow upstream of the stripper.

measured data. The carbon-capture rate is defined as the fraction of absorbed CO₂ out of the total CO₂ entering the absorption unit.

$$X_{\text{CO}_2} = 1 - \frac{\dot{N}_{\text{CO}_2, \text{Abs, out}}}{\dot{N}_{\text{CO}_2, \text{Abs, in}}} \quad (12)$$

In the pilot plant, the capture rate could not be calculated right from the beginning, as the CO₂ concentration at absorber flue-gas outlet could only be measured from time $t \approx 2000$ s. At the beginning, the solvent is not saturated in the absorption unit, and a significant amount of carbon dioxide can be captured. The carbon-capture rate is almost 1. When the solvent is saturated, the capture rate drops nearly instantaneously. Then, the model underestimates the minimum of the capture rate at $t \approx 5000$ s. At this time, because of the increasing temperatures in the reboiler and stripper, solvent regeneration is started. As a consequence, the carbon-capture rate increases slowly until the steady-state-capture rate of 90% is reached. The delay is caused by the high amount of solvent in the stripper sump that has to be regenerated. After the minimum, the model shows a very good agreement with measured values. The startup end time is predicted well by the model.

The CO₂-mass flow upstream of the stripper also shows good agreement with measured data. The beginning of the CO₂-mass flow is predicted very well. After $t \approx 5000$ s, a deviation in the simulation data can be seen as the slope of the mass flow is underpredicted in the model. At the end of the startup process, a larger overshoot of CO₂-mass flow can be seen in the simulation results. This is due to the assumption that the upstream steam fully condenses as long as the boiling point in the stage is not reached (step E in Figure 3). In reality, the CO₂ is loaded with steam when leaving the column. Therefore, the amount of condensing steam is lower. As a result, less energy can be provided for the regeneration of CO₂, and less CO₂ is desorbed in the pilot plant.

Figure 5 shows the pressure at the top of the stripper during startup. The stripper is initialized at ambient pressure. When the solvent evaporates in the reboiler, the pressure in the stripper increases. The pressure at the top is controlled using a control valve and is estimated well by the model, even though the pressure rise is much sharper. The slow pressure increase at the beginning cannot be represented by the model, as the pressure is set to ambient pressure until the boiling point in the reboiler is reached.

In Figure 6, the simulated temperature profiles of the absorption unit at different times are illustrated and compared to measured values. The intercooling section is located at a

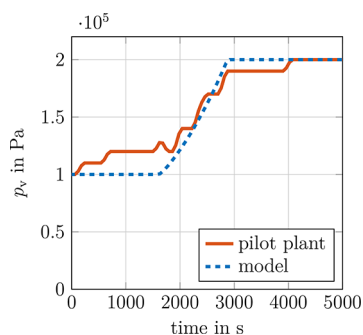


Figure 5. Comparison of pressures at stripper top during startup.

normalized height of 0.2. Below the intercooling section, the temperature was not measured in the plant. At each measuring point, the temperature is measured in the gas and liquid phases. Hence, two measurements are plotted at each time and height. The reaction in the absorption unit is exothermic. Consequently, the temperature is directly related to the amount of CO₂ reacting in this column section. At the beginning of the startup process, the reaction takes place in the lower section of the absorption unit. The reaction zone moves toward the upper section of the absorption unit over time. This phenomenon can be seen in the pilot plant and in the model, but the reaction zone in the model is separated sharply from the nonreaction zone. This can be clearly seen at time $t = 900$ s. It can be explained by the equilibrium approach that was used in the column, as the CO₂ reacts instantaneously with the solvent. Furthermore, mass transfer is not limited in the model, and the reaction kinetics are also neglected. The general shift of the temperature profile over time is well-predicted by the model. Nevertheless, the local temperatures are strongly underpredicted. The error increases over time and reaches its maximum at steady-state operation. This can be explained by an inaccuracy in the empirical correlation that is used to calculate the heat of reaction for the absorption reaction. The model developed by Wellner et al. to simulate the normal operation of the plant²¹ shows the same deviation. The equations in the absorber were not changed for the simulation of the startup process.

In Figure 7, the temperature profiles of the stripper at different times are shown. At first, the temperature increases in the reboiler. The stripper heats up in two different ways:

1. The vapor flow from the reboiler flows upstream through the stripper. The steam condenses, resulting in a temperature increase.
2. The rich solvent entering the stripper at the top is preheated by the lean solvent in the heat exchanger.

As a consequence, the lowest temperature in the stripper can be found in the central part of the column. The model slightly overpredicts the temperatures at $t = 2400$ and 3000 s, but the temperature profile at $t = 4800$ s shows very good agreement with measured temperatures, with the exception of the high deviation in the lower part of the stripper. The deviation can be explained by the numerical switching between steps E and F (see Figure 3) resulting in evaporation and condensation effects in the lowest column stage.

The temperature profile in steady-state operation fits the measured temperatures very well. Overall, the agreement of the measured and simulated temperature profiles is good.

Finally, it can be concluded that the simulation results correspond well to the measured data of the pilot plant. Therefore, the model can be used for further investigations in the following case study.

5. CASE STUDY

For the case study, a model of a pcc-plant at industrial scale is developed. The scale-up process is performed using a rigorous model developed with the simulation software Aspen Plus. The plant will handle the entire flue-gas flow of the 875 MW supercritical coal-fired power plant located in Heyden, Germany. The nominal flue-gas flow rate and flue-gas composition of the power plant are shown in Table S2 in the Supporting Information.

As packing material, the structured packing Mellapak 250Y is used.³² The diameters of these packings are limited to 15 m.³² Because of this restriction, the result of the scale-up process is three pcc-plants in parallel. Each plant can handle a nominal flue-gas flow of 320 kg/s. For the sake of simplification, only one of these pcc-plants is simulated in the following case study. In Table 2, the pcc-plant dimensions used for this case study are shown. It should be noted that it would also be possible to use only one stripper and three absorption units, because the gas loading in the stripper is much lower. The diameters of the columns are calculated in Aspen Plus by using the "fractional approach to maximum capacity". In this approach a specific factor has to be chosen. A factor of 1 would lead to a design

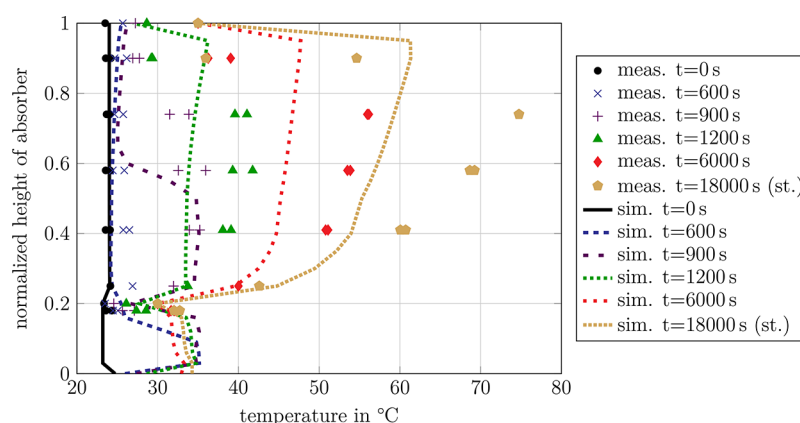


Figure 6. Temperature profile in the absorber at different times during startup (sim. = simulated results, meas. = measured pilot-plant values, st. = steady state).

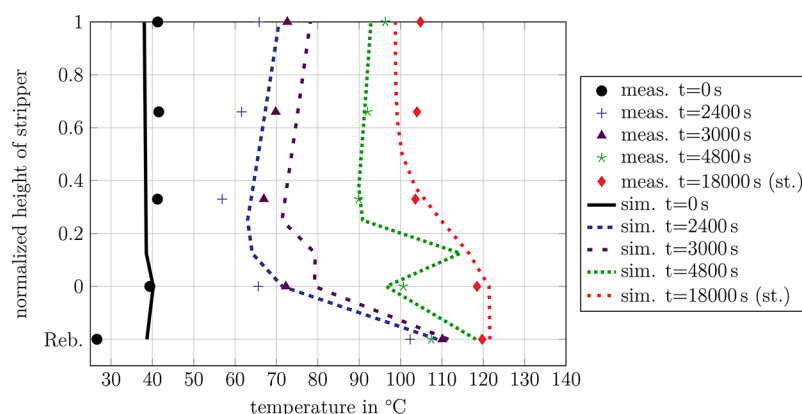


Figure 7. Temperature profiles in the stripper at different times during startup (sim. = simulated results, meas. = measured pilot-plant values, st. = steady state, Reb = reboiler).

Table 2. Overview of the Most Important Results of the Column Design

| | absorber | stripper |
|----------------|----------|------------------|
| amount | 3 | 3 (1) |
| diameter | 14.51 m | 8.51 m (14.80 m) |
| packing height | 15 m | 10 m |

directly at the flood point of the column. Therefore, a smaller factor is set to prevent the flooding of columns even at slightly higher gas or liquid loads. Agbonghae et al.³³ use a recommendation of Kister.³⁴ They recommend designing a packed column between 70 and 80% of the flood-point velocity. In this publication, a factor of 0.7 was chosen.

The heights of the columns were adapted manually. The goal was to achieve the same plant efficiency as in the pilot plant used for validation. The model is depicted in Figure 2.

The design data from Aspen Plus was implemented in the Modelica model, and the resulting model was used for the case study.

As the startup process has not been investigated in detail, different parameters and input variables in the model are varied, and their influence on startup time is investigated. All input variables and parameters are kept constant during each simulation run. For the case study, it is assumed that the power plant is operated in steady-state operation when the carbon-capture plant is started. The combined startup process with the power plant will be investigated in the future.

The startup is finished when the pcc-plant reaches a stable carbon-capture rate of 0.9 within an error band of 3%.

$$X_{\text{CO}_2, \text{end}} = 0.9 \pm 0.027 \text{ (3\%)} \quad (13)$$

In Figure 8, the startup times at different power-plant loads for a cold start and a warm start are illustrated. The stripper and reboiler temperatures for the warm start are assumed to be 80 °C. Because of the mixing of the solvent at the beginning of the startup process, the temperature decreases to approximately 65 °C when the steam flow into the reboiler is started.

The timer starts when the flue-gas flow into the absorption unit is started. The steam flow into the reboiler is started with a delay of $t = 240$ s. One hour before the flue-gas flow is started, the solvent pumps are switched on. The goal is to wet the columns and to achieve a homogeneous solvent composition. For the calculation of total startup time, this time span must be added to the startup times in Figure 8.

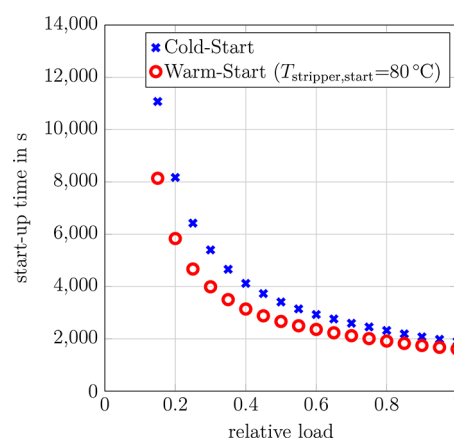


Figure 8. End time of startup when using steady-state input values at different power-plant loads.

All input variables (flue-gas flow rate, solvent flow rate, and steam flow rate) are kept constant at their corresponding steady-state values. More precisely, the flue-gas flow rate is set to the flue-gas flow rate of the power plant at the specific load. The solvent flow rate is constantly set to the optimal flow rate in steady-state operation. Finally, the steam flow rate is set to the amount that is needed to achieve a carbon-capture rate of 90% in steady-state operation at the corresponding load. The total amount of solvent is constant during all simulation runs.

As can be seen in Figure 8, the startup time increases exponentially with decreasing load. Starting from full load to approximately 50% load, the startup time increases almost linearly. At smaller loads below 40% load, the slope of the curve increases rapidly. As expected, the startup time of a warm startup is lower than the cold startup time. The absolute and relative time savings increase with decreasing partial load. The reason is that startup at high loads is limited by the amount of solvent that has to be replaced in the stripper sump, and the replacement rate is limited by the maximum solvent flow rate. At low partial loads, the startup process is limited by the slow heatup rate in the reboiler and stripper. Therefore, the higher temperature at the beginning has a larger impact on the startup time. Because of the increasing amount of renewable energies, it is expected that the operating time of power plants between two downtimes will decrease in the future. With regard to this matter, the startup of pcc-plants at low power-plant loads might be neither economically nor technically reasonable.

If the pcc-plant should also be operated at low power-plant loads, one possible solution would be to avoid the startup of the power plant and the pcc-plant during shorter downtimes. For this purpose, the operation of the power plant and the pcc-plant at a low minimum load must be possible. Therefore, future research should continue to focus on low-load operation of power plants and pcc-plants.

It is also possible to increase the steam extraction of the power plant at lower loads during startup, which would reduce the startup time, but this would also further reduce the power generation.

Besides the startup time, another important value for comparison is the total energy demand for the startup process. The highest energy demand is needed in the reboiler. As a consequence, the rest of the energy demand is neglected. The total heat required in the reboiler for startup is shown in Figure 9.

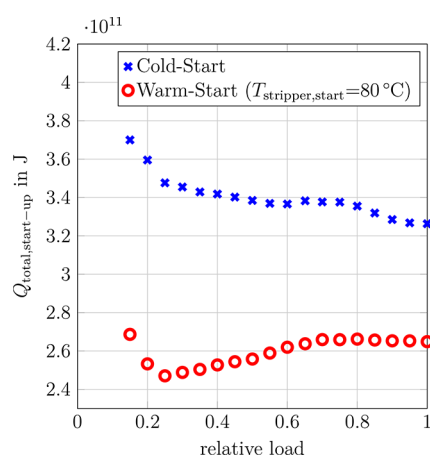


Figure 9. Total energy input into the reboiler during startup when using steady-state input values at different loads.

The total energy demand in the reboiler needed for a cold start decreases from lower loads to higher loads. In general, the results indicate that minimizing the startup time leads to lower energy consumption. Most of the energy losses during the startup process are induced by the terminal-temperature difference in the heat exchanger that is used to preheat the rich solvent coming from the absorption unit. This energy loss can be reduced by reducing the startup time. Hence, future research should focus on the minimization of startup time. An approach has already been developed²⁰ using an optimal solvent-flow trajectory that minimizes the startup time.

However, the total energy demand of a warm start up decreases slightly with decreasing load. Compared with a cold start, the startup is not limited by the heatup process in the reboiler and the stripper, but the startup is limited by the solvent in the stripper sump that has to be replaced. Therefore, a lower steam flow rate leads to energy savings. Only at very low partial loads does the energy demand increase again. For a warm start, 70–80% of the total energy demand of a cold start is required.

A large fraction of the energy is lost during the mixing of the solvent at the beginning of the startup process. This energy loss could be reduced by using shorter solvent-mixing times if possible. In this way, greater energy and time savings can be achieved. The minimal mixing time of the solvent required for stable operation can be determined (e.g., in pilot plants).

In Figure 10, the solvent flow rate is varied at different flue-gas loads. The steam flow into the reboiler is constantly set to its

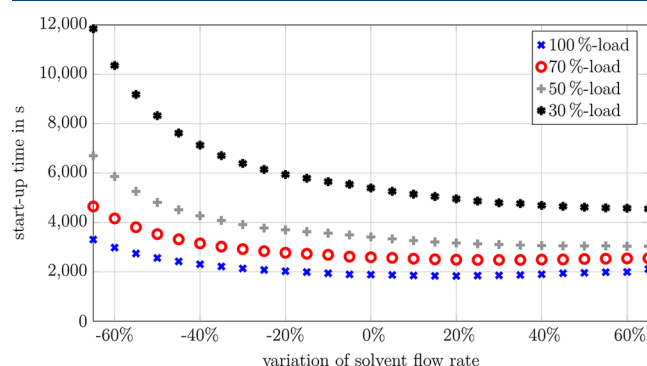


Figure 10. Endtime of the startup process when varying the solvent flow rate at different loads.

respective steady-state value. The solvent flow rate is also set to a constant value during one startup simulation and is only varied between different simulation runs. A variation of the solvent flow of 0% corresponds to the optimal steady-state value.

A reduction of the solvent flow rate always leads to an increase in startup time. An increase in solvent flow rate first reduces the startup time slightly, but a further increase results again in an increase in the startup time. It should be noted that a carbon-capture rate of 90% cannot be achieved after startup when the solvent flow rate is changed, as the process is not operated at the optimal operation point. Therefore, the startup is finished when the carbon-capture rate reaches the respective steady-state value within an error band of 3%.

Figure 11 shows the variation of the steam flow rate into the reboiler at different flue-gas loads. As a steady-state-carbon-

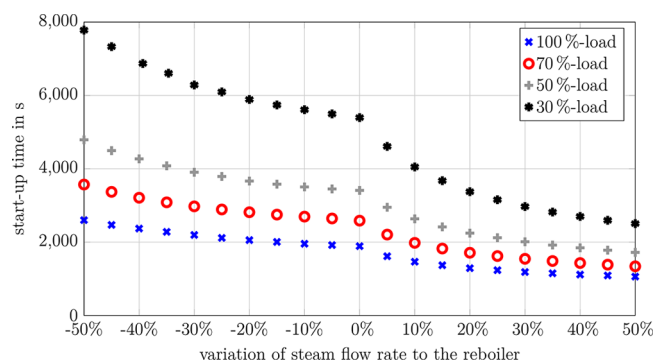


Figure 11. Endtime of the startup process when varying the steam flow rate into the reboiler at different loads.

capture rate of 90% cannot be achieved if the steam flow into the reboiler is reduced, the carbon-capture rate that indicates the end of the startup process is calculated in the following way:

$$X_{\text{CO}_2,\text{end}} = \min(0.9, X_{\text{CO}_2,\text{st}}) \pm (3\%) \quad (14)$$

The solvent flow rate is set to the optimal steady-state value in all cases. As expected, the startup time decreases with increasing steam flow rate. An increase in the steam flow rate above 50% does not further improve the startup time significantly. Worth of note, a small increase in the steam flow results in a significant reduction of the startup time, especially at partial loads. Hence, it could be desirable to start up the pcc-plant with additional steam

from the power plant. One drawback is that the steam flow into the reboiler has to be reduced after startup, leading to a disturbance in the reboiler, which has to be adjusted by the control system.

In Figure 12, the variation of the total amount of solvent in the plant is depicted. The increase or reduction of the total amount

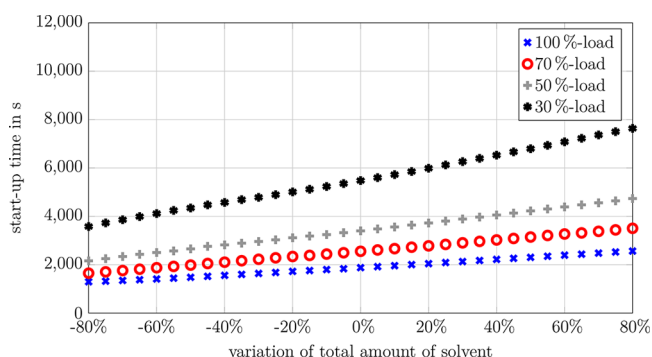


Figure 12. Endtime of the startup process when varying the total amount of solvent at different loads.

of solvent is evenly reduced or increased in the absorber and stripper sump. The startup time increases linearly in all cases. This can be explained by the higher amount of solvent in the stripper sump that has to be regenerated during startup. Only the slope differs between different loads. For a fast startup, it can be concluded that the total amount of solvent should stay as low as possible, still allowing safe and stable plant operation.

In Figure 13, different possible distributions of the solvent are presented. In the first three cases on the left side, the total

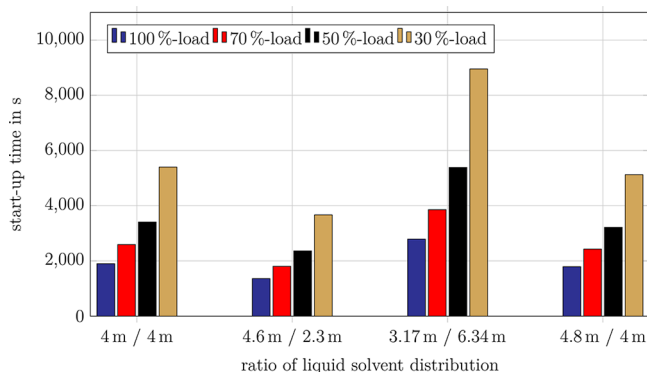


Figure 13. Comparison of startup times when using different solvent distributions (level of absorber sump/level of stripper sump).

amount of solvent in the plant is not changed. The solvent is only distributed differently over both column sumps. The ratio between both sumps can be seen in the diagram. The case on the left refers to the standard case in the figures above. The results confirm the assumption that a high amount of solvent in the stripper sump increases the startup time. This links well with the results by Tait et al.,³⁵ who concluded that a larger total amount of solvent leads to a longer stabilization time of the plant.³⁶

In the case on the right side of Figure 13, the total amount of solvent in the stripper sump remains constant, and only the amount of solvent in the absorption sump is increased. It can be seen that the startup time decreases slightly in this case. This effect is explained below.

At the beginning of the startup process, when the flue gas enters the absorber, the solvent loading in the absorber increases. Consequently, the solvent loading in the absorption sump increases slowly. The rich solvent is transported to the stripper sump, where the solvent cannot be regenerated yet. Therefore, the solvent loading in the stripper sump also increases. To illustrate this, the solvent loadings in the stripper sump (lean loading) and the absorption sump (rich loading) are shown in Figure 14 for both absorption-sump levels (4.8 and 4

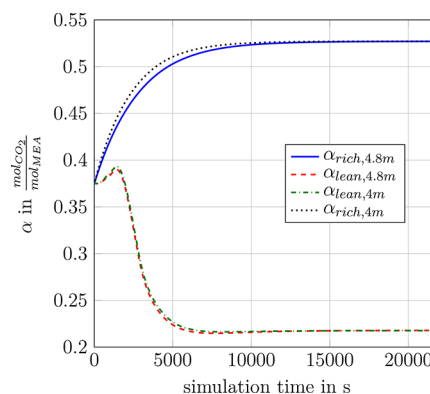


Figure 14. Comparison of rich- and lean-solvent loadings during startup with different absorption-sump levels.

m) during a startup at a partial load of 30%. Because of the greater amount of solvent in the absorption sump, the rich-solvent loading increases more slowly when the absorption-sump level is higher. Hence, also the lean loading increases more slowly, and it takes less time to reach the desired lean-solvent loading after startup.

It can be concluded that a high amount of solvent in the absorption sump reduces the startup time, whereas a high amount of solvent in the stripper sump increases the startup time.

6. MODEL APPLICATION FOR PROCESS IMPROVEMENT

In the parameter study above, the influence of different input variables and parameters is investigated. In this section, the model is used to test two different process configurations in order to improve the operation of the startup process. At the end of the section, all recommendations on how to run the startup process are summarized. The results show how the model can be used to improve the process operation.

6.1. Using an Additional Lean-Solvent Tank for Startup. In the first test case, an additional solvent tank on the lean-solvent side is used to start up the absorption unit. The solvent tank is filled with regenerated lean solvent that can be used to control the capture rate during startup. The stripper is started simultaneously. An additional pump is used to control the capture rate during startup using the volume flow of fresh, regenerated solvent, which is mixed with the solvent coming from the stripper sump. The additional solvent is then stored in the absorption sump until the startup in the stripper is finished. The additional solvent has to be regenerated after startup, and the additional solvent tank has to be refilled for the next startup. The aim is to achieve a carbon-capture rate of 90% during the heatup process of the stripper. With the model, the dimensions of this solvent tank can be designed, and the needed amount of additional regenerated solvent can be calculated.

Figure 15 shows the carbon-capture rate for a cold start at full load in the reference case compared with that of the test case. It

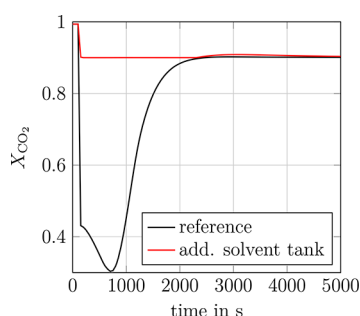


Figure 15. Carbon-capture rate during startup in the reference case and in test case 1 (additional lean-solvent tank).

can be seen that a carbon-capture rate of 90% can be achieved during the complete startup process.

The drawback when using an additional solvent tank is that the additional solvent has to be regenerated after startup for use in the next startup. The additional solvent needed for the startup is approximately 750 m³ at full load and reduces with reducing load until a minimum of 450 m³ at 15% load. The advantage is that a carbon-capture rate of at least 90% can be achieved directly at power-plant startup.

For the regeneration of the solvent, additional steam from the power plant has to be used. If the steam extraction is increased by 10% at full load after startup, it would take 2.4 h to regenerate the additional solvent. At a partial load of 15%, an increase of 10% would lead to a regeneration time of 9.2 h. However, it is unlikely that the power-plant load does not increase after startup in most cases. Therefore, the regeneration of the additional solvent can also be performed later at higher loads, resulting in lower regeneration times. The total amount of additional solvent that is needed for the startup is lower at partial loads, which is a great advantage.

6.2. Startup with Variable Stripper Pressure. In the second test case, the stripper pressure is no longer fixed at 2 bar. A control valve is used to control the stripper pressure after the condenser. The advantage is that an additional degree of freedom is created for the control system. In this short test case, it is proved that a variable stripper pressure has an influence on the startup time.

When the solvent evaporates in the reboiler the pressure at the stripper first increases from ambient pressure to 1.5 bar in this test case. After startup, the stripper pressure is slowly increased to 2 bar. In the reference case, the pressure directly increases up to 2 bar.

Figure 16 compares the carbon-capture rates in the reference case and in the second test case.

It can be concluded that the startup time decreases because of the variable stripper pressure and that the carbon-capture rate is only slightly affected by the disturbance. The time saving is 116 s.

At low partial loads, reducing the stripper pressure during startup has a negative effect on the startup. Therefore, the best stripper pressure during startup depends on the load of the power plant. The model can be used to find the optimal stripper pressure for startup and guarantee a smooth transition between the stripper pressure during startup and the optimal operation pressure afterward.

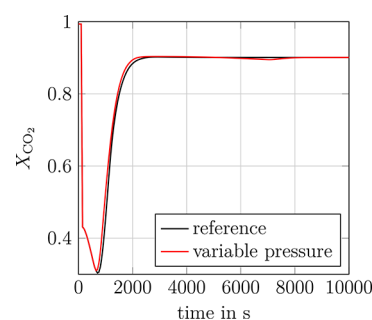


Figure 16. Carbon-capture rate during startup in the reference case and in test case 2 (variable stripper pressure).

6.3. Recommendations for Process Operation. Finally, the recommendations made in these test cases and the case study in the section above will be summarized. The following recommendations for the operation of the startup process are given by the authors:

- Avoid startup processes by improving the ability of the power plant to operate at very low partial loads.
- Use the optimal solvent-flow-rate trajectory for the startup to decrease the startup time, as shown in a previous publication.²⁰
- Keep the total amount of solvent in the stripper sump as low as technically possible. (Using forced circulation in the reboiler instead of natural circulation can reduce the needed solvent on the lean-solvent side.)
- Slightly increase the steam flow into the reboiler during startup to achieve a much lower startup time (as can be seen in Figure 11).
- Introduce an additional degree of freedom by using a variable stripper pressure.
- Use an additional lean-solvent tank for the startup of the absorber to achieve a carbon-capture rate of at least 90% during the complete startup.

7. CONCLUSION AND OUTLOOK

In this work a startup model of a postcombustion-capture plant is developed and validated with measured data of a pilot plant in Heilbronn, Germany. The validation results show good agreement with measured data. After validation, the pcc-plant model is scaled up to the industrial scale. Different parameters and input variables are varied for an in-depth analysis of the process.

The results show that the startup time increases drastically when the pcc-plant is started up at low partial loads of the power plant. The startup time first increases almost linearly with decreasing load for loads above 50%. For lower loads, the startup time increases enormously. In the case of a cold start from beginning steam flow to a 90% carbon-capture rate, the startup time increases by 79% at 50% load and by 480% at 15% load compared with the startup time at full load. The total energy demand increases only slightly by 13% at 15% load compared with that of the full-load startup. The additional results of the case study show the influences of different plant parameters and input variables. When the startup is performed with a constant solvent flow rate, the optimal solvent flow rate during regular operation is not the optimal solvent flow rate in terms of the startup time. In the last section, the potential of the model to improve the startup process is shown. By using an additional solvent tank, it is possible to achieve a carbon-capture rate of at

least 90% during startup. A variable stripper pressure can be used to reduce the startup time. In the last section, the potential of the model for improving the process operation is shown. In particular, the introduction of an additional solvent tank is a very good option for reducing the carbon emissions.

In the future, it will be desirable to use the model in an optimization algorithm to find the optimal startup process in terms of low cost, low emission, or low energy demand for different boundary conditions. From a plant-operator point of view, minimizing the costs will be the most desirable task. However, the results in this publication indicate that minimizing the startup time also has a lot of benefits. Minimizing the startup time does not guarantee that the costs or the CO₂ emissions are the lowest possible, but a fast startup guarantees that a high carbon-capture rate is achieved as fast as possible. In the case of a cold start, Figure 9 shows that the energy demand for startup increases with increasing startup time, which reduces a high percentage of costs. Furthermore, a fast startup is also useful to reduce the influence on the power plant, as the steam flow to the reboiler is stabilized after startup.

Furthermore, future research should concentrate on low-partial-load operation of power plants with pcc during shorter downtimes to avoid startup processes. In addition, the pcc-plant model can be coupled to a model of a thermal power plant to investigate the interactions between the plants during startup. The coupled model can be used to develop appropriate control structures for an efficient combined-startup operation.

■ ASSOCIATED CONTENT

Supporting Information

The Supporting Information is available free of charge on the ACS Publications website at DOI: 10.1021/acs.iecr.8b03444.

Overview of the varied equations during stripper startup and flue-gas parameters used for the case study (PDF)

■ AUTHOR INFORMATION

Corresponding Author

*E-mail: thomas.marx@tuhh.de. Tel.: +49 (0)40 42878-3144. Fax: +49 (0)40 42878-2632.

ORCID

Thomas Marx-Schubach: 0000-0001-8840-5528

Notes

The authors declare no competing financial interest.

■ ACKNOWLEDGMENTS

This research project has been supported by the German Federal Ministry for Economic Affairs and Energy (project number 03ET7060B), which is greatly acknowledged.

■ NOMENCLATURE

α = solvent loading (mol_{CO₂}/mol_{MEA})
 \dot{m} = mass flow rate (kg/h)
 \dot{N} = mole flow rate (mol/h)
 \dot{Q} = heat flow rate (W)
 b = molality
 c = molar concentration
 n = amount of substance
 p = pressure (mbar, bar, or Pa)
 Q = amount of heat (J)
 T = temperature (°C or K)
 t = time (s)

X = CO₂ capture rate (%)
 x = mole fraction
 CCS = carbon capture and storage
 MEA = monoethanolamine
 PCC = postcombustion carbon capture
 * = composition at the phase boundary
 abs = absorber
 end = indicates the end of the startup process
 F = feed
 HU = holdup
 i = index for component
 init = initial value
 j = stage
 K = calibration factor for approximate equilibrium condition
 L = liquid phase
 lean = CO₂ lean condition
 Reb = reboiler
 rich = CO₂ rich condition
 st = steady-state value
 str = stripper
 sys = system
 trans = transferred over the phase boundary
 V = vapor phase
 vap = vapor flow

■ REFERENCES

- (1) Leung, D. Y.; Caramanna, G.; Maroto-Valer, M. M. An overview of current status of carbon dioxide capture and storage technologies. *Renewable Sustainable Energy Rev.* **2014**, *39*, 426–443.
- (2) Rochelle, G. T. Amine scrubbing for CO₂ capture. *Science (Washington, DC, U. S.)* **2009**, *325*, 1652–1654.
- (3) Montañés, R. M.; Korpás, M.; Nord, L. O.; Jaehnert, S. Identifying Operational Requirements for Flexible CCS Power Plant in Future Energy Systems. *Energy Procedia* **2016**, *86*, 22–31.
- (4) Bui, M.; Gunawan, I.; Verheyen, V.; Feron, P.; Meuleman, E.; Adeboju, S. Dynamic modelling and optimization of flexible operation in post-combustion CO₂ capture plants—A review. *Comput. Chem. Eng.* **2014**, *61*, 245–265.
- (5) Kvamsdal, H. M.; Rochelle, G. T. Effects of the Temperature Bulge in CO₂ Absorption from Flue Gas by Aqueous Monoethanolamine. *Ind. Eng. Chem. Res.* **2008**, *47*, 867–875.
- (6) Ruiz, C. A.; Cameron, I. T.; Gani, R. A Generalized Dynamic Model for Distillation Columns - III. Study of Startup Operations. *Comput. Chem. Eng.* **1988**, *12*, 1–14.
- (7) Cameron, I. T.; Ruiz, C. A.; Gani, R. A generalized model for distillation columns—I: Model Description and Applications. *Comput. Chem. Eng.* **1986**, *10*, 199–211.
- (8) Kruse, C.; Fieg, G.; Wozny, G. Entwicklung und experimentelle Absicherung eines Simulationsprogrammes für Anfahrvorgänge an Rektifikationskolonnen [Development and experimental validation of a simulation tool for distillation column start-up] (In German). *Heat Mass Transfer* **1995**, *31*, 25–31.
- (9) Wang, L.; Li, P.; Wozny, G.; Wang, S. A startup model for simulation of batch distillation starting from a cold state. *Comput. Chem. Eng.* **2003**, *27*, 1485–1497.
- (10) Dietl, K. Equation-Based Object-Oriented Modelling of Dynamic Absorption and Rectification Processes. Ph.D. Thesis, Hamburg University of Technology, Hamburg, 2012.
- (11) Reepmeyer, F.; Repke, J.-U.; Wozny, G. Time optimal start-up strategies for reactive distillation columns. *Chem. Eng. Sci.* **2004**, *59*, 4339–4347.
- (12) Forner, Florian Anfahren von Reaktivrektifikationsprozessen in Kolonnen mit unterschiedlichen Einbauten [Start-Up of reactive rectification processes in columns with different column internals] (in German). Ph.D. Thesis, Technical University of Berlin, 2008.

- (13) Forner, F.; Brehelin, M.; Rouzineau, D.; Meyer, M.; Repke, J.-U. Startup of a reactive distillation process with a decanter. *Chem. Eng. Process.* **2008**, *47*, 1976–1985.
- (14) Elgue, S.; Prat, L.; Cabassud, M.; Le Lann, J. M.; Cézerac, J. Dynamic models for start-up operations of batch distillation columns with experimental validation. *Comput. Chem. Eng.* **2004**, *28*, 2735–2747.
- (15) Niggemann, G.; Hiller, C.; Fieg, G. Modeling and in-depth analysis of the start-up of dividing-wall columns. *Chem. Eng. Sci.* **2011**, *66*, 5268–5283.
- (16) Jayarathna, S. A.; Lie, B.; Melaaen, M. C. Dynamic modelling of the absorber of a post-combustion CO₂ capture plant: Modelling and simulations. *Comput. Chem. Eng.* **2013**, *53*, 178–189.
- (17) Kvamsdal, H. M.; Jakobsen, J. P.; Hoff, K. A. Dynamic modeling and simulation of a CO₂ absorber column for post-combustion CO₂ capture. *Chem. Eng. Process.* **2009**, *48*, 135–144.
- (18) Wellner, K. C. Simulation des dynamischen Verhaltens von thermischen Trennprozessen am Beispiel der CO₂-Abtrennung [Simulation of the dynamic behaviour of thermal separation processes using the carbon capture process as an example] (in German). Ph.D. Thesis, Hamburg University of Technology, Hamburg, 2016.
- (19) Gaspar, J.; Jorgensen, J. B.; Fosbol, P. L. Control of a post-combustion CO₂ capture plant during process start-up and load variations. *IFAC-PapersOnLine* **2015**, *48*, 580–585.
- (20) Marx-Schubach, T.; Schmitz, G. Optimizing the start-up process of post-combustion capture plants by varying the solvent flow rate. *Proceedings of the 12th International Modelica Conference*, Prague, Czech Republic, May 15–17, 2017; Linköping University Electronic Press, 2017; pp 121–130.
- (21) Wellner, K.; Marx-Schubach, T.; Schmitz, G. Dynamic Behavior of Coal-Fired Power Plants with Postcombustion CO₂ Capture. *Ind. Eng. Chem. Res.* **2016**, *55*, 12038–12045.
- (22) Modelica — A Unified Object-Oriented Language for Systems Modeling: Language Specification Version 3.4, 2017. *Modelica Association*. <https://www.modelica.org/documents/ModelicaSpec34.pdf>.
- (23) ClaRa⁺ — Power Plant Simulation. <http://www.claralib.com>.
- (24) Thermal Power Library. *Modelon*. <http://www.modelon.com/products/modelica-libraries/thermal-power-library/>.
- (25) Gardarsdóttir, S. Ó; Montañés, R. M.; Normann, F.; Nord, L. O.; Johnsson, F. Effects of CO₂ -Absorption Control Strategies on the Dynamic Performance of a Supercritical Pulverized-Coal-Fired Power Plant. *Ind. Eng. Chem. Res.* **2017**, *56*, 4415–4430.
- (26) Joos, A.; Dietl, K.; Schmitz, G. Thermal Separation: An Approach for a Modelica Library for Absorption, Adsorption and Rectification. *Proceedings of the 7th International Modelica Conference*, Como, Italy, Sept 20–22, 2009; Linköping University Electronic Press, 2009; pp 804–813.
- (27) Oexmann, J. *Post-combustion CO₂ capture: Energetic evaluation of chemical absorption processes in coal-fired steam power plants*, 1st ed.; Cuvillier: Göttingen, 2011.
- (28) Stichlmair, J.; Bravo, J. L.; Fair, J. R. General model for prediction of pressure drop and capacity of countercurrent gas/liquid packed columns. *Gas Sep. Purif.* **1989**, *3*, 19–28.
- (29) Dietl, K.; Joos, A.; Schmitz, G. Dynamic analysis of the absorption/desorption loop of a carbon capture plant using an object-oriented approach. *Chem. Eng. Process.* **2012**, *52*, 132–139.
- (30) Metal random packings. *Vereinigte Füllkörper-Fabriken GmbH & Co. KG*. <https://www.vff.com/en/products/random-packings/metals>.
- (31) Rieder, A.; Unterberger, S. EnBW's post-combustion capture pilot plant at Heilbronn - Results of the first year's testing programme. *Energy Procedia* **2013**, *37*, 6464–6472.
- (32) Structured Packings for Distillation, Absorption and Reactive Distillation, 2018. *Sulzer Chemtech*. http://www.sulzer.com/-/media/files/products/separation-technology/distillation-and-absorption/brochures/structured_packings.ashx.
- (33) Agbonghae, E. O.; Hughes, K. J.; Ingham, D. B.; Ma, L.; Pourkashanian, M. Optimal Process Design of Commercial-Scale Amine-Based CO₂ Capture Plants. *Ind. Eng. Chem. Res.* **2014**, *53*, 14815–14829.
- (34) Kister, H. Z. *Distillation design*; McGraw Hill: New York, 1992.
- (35) Tait, P.; Buschle, B.; Ausner, I.; Valluri, P.; Wehrli, M.; Lucquiaud, M. A pilot-scale study of dynamic response scenarios for the flexible operation of post-combustion CO₂ capture. *Int. J. Greenhouse Gas Control* **2016**, *48*, 216–233.
- (36) Montañés, R. M.; Flø, N. E.; Nord, L. O. Experimental results of transient testing at the amine plant at Technology Centre Mongstad: Open-loop responses and performance of decentralized control structures for load changes. *Int. J. Greenhouse Gas Control* **2018**, *73*, 42–59.